Article

Combined NMR and DFT Studies for the Absolute Configuration Elucidation of the Spore Photoproduct, a UV-Induced DNA Lesion

Claire Mantel, Alexia Chandor, Didier Gasparutto, Thierry Douki, Mohamed Atta, Marc Fontecave, Pierre-Alain Bayle, Jean-Marie Mouesca, and Michel Bardet

J. Am. Chem. Soc., **2008**, 130 (50), 16978-16984 • DOI: 10.1021/ja805032r • Publication Date (Web): 14 November 2008

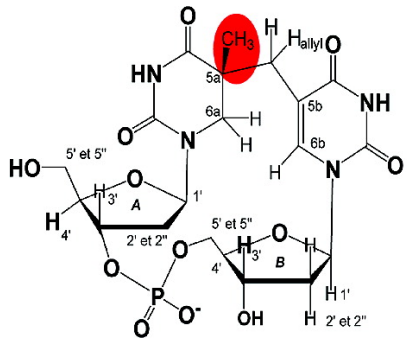

R isomer of SPTpT

More About This Article

Additional resources and features associated with this article are available within the HTML version:

- Supporting Information
- Access to high resolution figures
- Links to articles and content related to this article
- Copyright permission to reproduce figures and/or text from this article

View the Full Text HTML

J|A|C|S
ARTICLES

Published on Web 11/14/2008

Combined NMR and DFT Studies for the Absolute Configuration Elucidation of the Spore Photoproduct, a UV-Induced DNA Lesion

Claire Mantel,[§] Alexia Chandor,[†,‡] Didier Gasparutto,[†] Thierry Douki,[†] Mohamed Atta,[‡] Marc Fontecave,[‡] Pierre-Alain Bayle,[§] Jean-Marie Mouesca,*[,§] and Michel Bardet*[,§]

CEA, INAC, SCIB, F-38054 Grenoble, France, and CEA, IRTSV, F-38054 Grenoble, France

Received July 1, 2008; E-mail: jean-marie.mouesca@cea.fr; michel.bardet@cea.fr

Abstract: By irradiation of bacterial spores under UV radiation, a photoproduct (SP) bearing a covalent methylene link between two adjacent thymines is formed in DNA. Because of the presence of an asymmetric carbon on the aglycone and of two possible orientations for the formation of the cross-link, four isomers could in principle be obtained. Currently, no conclusive structural information of this photoproduct is available. The structure of the isolated SPTpT dinucleotide was revisited in order to determine the type of cross-link and the absolute configuration of the C_{5a} carbon. For this purpose, a study combining NMR spectroscopy and DFT calculations was pursued on the spore photoproduct of the dinucleoside TpT since its structure was previously shown to be identical to the one produced in DNA. A full characterization of SPTpT by NMR analyses was performed in D_2O and DMSO. 2D NMR measurements ($^1H-^{13}C$, $^1H-^{31}P$, COSY, NOESY, and ROESY) and DFT calculations (geometries optimization of *R* and *S* isomers and theoretical chemical shifts) lead us to conclude without ambiguity that the absolute configuration of the C_{5a} carbon is *R* and that the methylene bridge of the photoproduct corresponds to the methyl group of the thymine located on the 3′-end of the dinucleoside monophosphate.

Introduction

UVB and UVC radiation (190−280 nm) exhibit strong mutagenic and carcinogenic effects that are mostly explained by cellular DNA absorption.[1,2] The photochemical excitation results in the dimerization of adjacent pyrimidines. In eukaryotic and vegetative prokaryotic cells, such photoproducts can be classified into two classes, the cyclobutane pyrimidine dimers and the pyrimidine (6−4) photoproducts. By contrast, UV irradiation of bacterial spores leads to the sole formation of a photoproduct involving two thymines: 5-(α-thyminyl)-5,6-dihydrothymine, the so-called spore photoproduct (SP). The formation and the repair[3−8] of this photoproduct has already been studied extensively over the last 40 years, but the 3D structure of the compound and its absolute configuration still need to be understood. Two types of SPTpT dinucleotide lesions can be theoretically obtained: (1) a dinucleotide, dubbed 5′→ 3′, in which the base containing the unmodified methyl group at carbon C_{5a} appears first when reading the DNA sequence from the 5′→ 3′ carbons; (2) a dinucleotide, dubbed 3′→ 5′, in which it appears second (respectively Figures 1A and 1B). Furthermore, during formation of the lesion, a chiral center is generated at carbon C_{5a}, which thus can adopt either an *R* or *S* configuration. Therefore, depending on the type of cross-link and the stereochemistry of carbon C_{5a}, the possible stereoisomers number stands at four (Figure 1). Only a limited amount of work has been devoted to answer this question. Using an elegant total synthesis, Begley et al.[9] obtained two diastereoisomers of the 5′ → 3′ SP as a dinucleoside monophosphate (here noted SPTpT) (Figure 1A, isomers *R* and S). NMR characterization of both diastereoisomers was carried out. However, lack of comparison with the natural SP precluded any definitive conclusion on the stereoconfiguration of this last photoproduct. More recently, Carrell et al.[10] determined the configuration of two other SP dinucleoside analogues: the thymidine derivative without the phosphodiester bridge, and a dinucleoside dimer where sugar units were linked through an alkyl chain.

In this work, we reinvestigated the structure of SPTpT to determine the absolute configuration of the natural SP by combining NMR measurements and theoretical DFT calculations. For that purpose, SPTpT was produced by irradiation of the unmodified thymine-thymine dinucleoside monophosphate.

[§] CEA, INAC, SCIB UMR-E 3 CEA-UJF, Laboratoire de Résonance Magnétique.
[†] CEA, INAC, SCIB UMR-E 3 CEA-UJF, Laboratoire "Lésions des Acides Nucléiques.
[‡] CEA, IRTSV, Laboratoire Chimie et Biologie des Métaux.

(1) Begley, T. P. *Acc. Chem. Res.* **1994**, *27*, 394–401.
(2) Sancar, A. *Biochemistry* **1994**, *33*, 2–9.
(3) Donnella, Je; Setlow, R. B. *Science* **1965**, *149*, 308–310.
(4) Varghese, A. J. *Biochem. Biophys. Res. Commun.* **1970**, *38*, 484–490.
(5) Munakata, N.; Rupert, C. S. *J. Bacteriol.* **1972**, *11*, 192–198.
(6) Slieman, T. A.; Rebeil, R.; Nicholson, W. L. *J. Bacteriol.* **2000**, *182*, 6412–6417.
(7) Cheek, J.; Broderick, J. B. *J. Am. Chem. Soc.* **2002**, *124*, 2860–2861.
(8) Chandor, A.; Berteau, O.; Douki, T.; Gasparutto, D.; Sanakis, Y.; Ollagnier-De-Choudens, S.; Atta, M.; Fontecave, M. *J. Biol. Chem.* **2006**, *281*, 26922–26931.
(9) Kim, S. J.; Lester, C.; Begley, T. P. *J. Org. Chem.* **1995**, *60*, 6256–6257.
(10) Friedel, M. G.; Pieck, J. C.; Klages, J.; Dauth, C.; Kessler, H.; Carell, T. *Chem.—Eur. J.* **2006**, *12*, 6081–6094.

10.1021/ja805032r CCC: $40.75

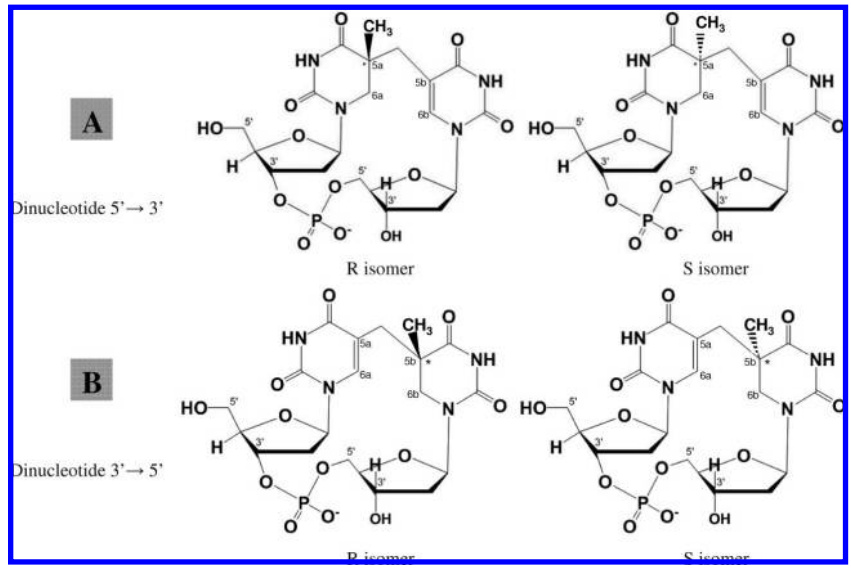

Figure 1. Representation of the two types of SPTpT lesions (A and B) and of their two respective *R* and *S* isomers.

HPLC−mass spectrometry characterization and ^{1}H NMR spectrum had previously shown[8] that only one product was obtained in this way. Furthermore, HPLC retention time and fragmentation mass spectrometry features of that compound were found to be identical to the SPTpT enzymatically released from DNA extracted from UV-irradiated spores.[8] The present work unambiguously demonstrates that this natural SPTpT compound is the dinucleotide 5′→3′ with an *R* configuration at carbon C_{5a} (Figure 1A, *R* isomer).

Experimental Section

Preparation of SPTpT. SPTpT was prepared by exposure of dry films of TpT and dipicolinic acid (DPA) to UVC radiations. For this purpose, 300 mL of 1 mM TpT solution containing 10 mM DPA under its sodium form (pH 7) was prepared. The solution was divided in six equal fractions that were poured in six 15 cm diameter Petri dishes and freeze-dried overnight. The dry films were then exposed for 1 h to UVC light emitted by a germicidal lamp (254 nm). The dry residues were made soluble in 30 mL of water. The freeze-drying/irradiation/solubilization cycle was repeated six times. After the last irradiation, the whole dry residue was made soluble in 10 mL of water. SPTpT was isolated by reverse phase HPLC in the gradient mode by using triethylammonium acetate (pH 6.5) and acetonitrile as solvents. Identity and purity of the collected photoproduct were inferred from the comparison of its HPLC-MS/MS features (Figure S4 in Supporting Informations) with those of authentic SPTpT isolated from DNA.

NMR Spectroscopy. 1D and 2D spectra were recorded on a Bruker Avance 500 spectrometer at a variable temperature (between 278 and 298 K) using a 5 mm indirect detection probe. ^{1}H and ^{13}C chemical shifts were referenced to D_2O and DMSO. The 1D ^{13}C spectrum in D_2O was recorded on a Varian Unity 400 MHz spectrometer. 2D-NMR experiments ^{1}H−^{1}H COSY, TOCSY, ^{1}H−^{13}C HSQC, ^{1}H−^{13}C HMBC, ^{1}H−^{31}P HMBC, NOESY, and ROESY were performed using the standard Bruker pulse sequences. The mixing times for the NOESY and ROESY experiments were between 50 ms and 1 s. For the ROESY experiments, a moderate spin lock pulse ($\gamma B_1/2\pi$) was used with field strength of 2126 Hz. In order to eliminate the signal of DMSO, weft-ROESY (typically used to remove the NMR signal of residual water) experiments were achieved. The SPTpT product was dissolved in deuterated water (D_2O) or in deuterated dimethyl sulfoxide ($(CD_3)_2SO$).

Theoretical Calculations. Molecular mechanics calculations were made with COSMOS 5.0 Pro-Version software.[11−13] For each configuration, two calculations were carried out in ten thousand steps and geometries were registered every hundred steps. Following these calculations, for both diastereoisomers, the two geometries of lowest energies were stored and used for further geometry optimization by DFT means. DFT calculations relied on the LCAO-ADF (Amsterdam Density Functional 2006) code developed by Te Velde and Baerends.[14−19] They include the VBP exchange-correlation potential (Vosko, Wilk, and Nusair exchange-correlation energy[20,21]) completed by nonlocal gradient corrections to the exchange by Becke[22] and to the correlation by Perdew.[23] We used triple-ζ (plus polarization) basis sets for all atoms, the numerical accuracy parameter being set to 6.0. We further relied on the ADF NMR subroutine for the computations of NMR shielding tensors and corresponding isotropic values (σ_i). The reference shielding values σ_{REF} for the ^{1}H and ^{13}C nuclei were set at 31.3 ppm and 176.9 ppm, respectively, and the NMR chemical shifts (δ_i) were computed as $\delta_i = \sigma_{REF} - \sigma_i$.

Results

Structure Determination of the SPTpT by NMR Experiments in D_2O. As SPTpT is a nucleic acid derivative, the structure was first studied in aqueous solution. Solubility was not a concern because the phosphodiester bridge makes the compound highly soluble in D_2O. The assignments of most of the ^{1}H and ^{13}C NMR signals were obtained by combining results from proton−proton COSY (through-bond correlation), proton−

(11) Sternberg, U. *Mol. Phys.* **1988**, *63*, 249–267.
(12) Sternberg, U.; Koch, F. T.; Mollhoff, M. *J. Comput. Chem.* **1994**, *15*, 524–531.
(13) Sternberg, U.; Koch, F. T.; Brauer, M.; Kunert, M.; Anders, E. *J. Mol. Model.* **2001**, *7*, 54–64.
(14) Baerends, E. J.; Ellis, D. E.; Ros, P. *Chem. Phys.* **1973**, *2*, 41–51.
(15) Baerends, E. J.; Ros, P. *Chem. Phys.* **1973**, *2*, 52–59.
(16) Baerends, E. J.; Ros, P. *Int. J. Quantum Chem.* **1978**, 169–190.
(17) Bickelhaupt, F. M.; Baerends, E. J.; Ravenek, W. *Inorg. Chem.* **1990**, *29*, 350–354.
(18) Velde, G. T.; Baerends, E. J. *J. Comput. Phys.* **1992**, *99*, 84–98.
(19) Ziegler, T. *Chem. Rev.* **1991**, *91*, 651–667.
(20) Painter, G. S. *J. Phys. Chem.* **1986**, *90*, 5530–5535.
(21) Vosko, S. H.; Wilk, L.; Nusair, M. *Can. J. Phys.* **1980**, *58*, 1200–1211.
(22) Becke, A. D. *Phys. Rev. A* **1988**, *38*, 3098–3100.
(23) Perdew, J. P.; Yue, W. *Phys. Rev. B* **1986**, *33*, 8800–8802.

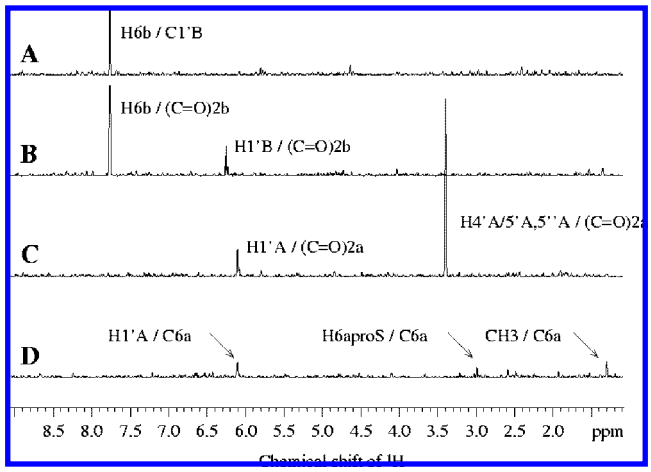

Figure 2. Extracted row from $^{1}H-^{13}C$ HMBC of the dinucleotide spore photoproduct SPTpT diluted in D_2O. A: Row corresponding to the $C_{1'B}$ coupling; B: Row corresponding to the $(C{=}O)_{2b}$ coupling; C: Row corresponding to the $(C{=}O)_{2a}$ coupling; D: Row corresponding to the C_{6a} coupling.

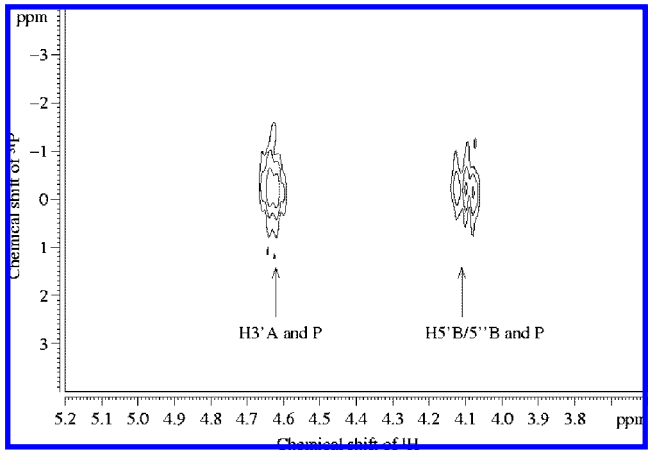

Figure 3. $^{1}H-^{31}P$ HMBC of the dinucleotide spore photoproduct SPTpT diluted in D_2O. The correlations are indicated by the arrows.

proton NOESY (through space correlation), proton−carbon HSQC ($^{1}J_{CH}$ coupling), and HMBC ($^{2,3}J_{CH}$ coupling) and proton−phosphate HSQC ($^{1}J_{PH}$ coupling) experiments. The assignments of the different signals are reported in Table S1 of Supporting Informations together with the relevant correlations on which they rely. To avoid confusing numbering, the four protons belonging either to CH_2 of the base or to bridging CH_2 were directly denoted with their final assignments, namely respectively $H_{6apro\mathit{R}}/H_{6apro\mathit{S}}$ and $H_{pro\mathit{R}}/H_{pro\mathit{S}}$. The proton−carbon and proton−phosphate correlations obtained from the 2D NMR experiments in D_2O allowed us to unambiguously determine how the bases and sugars are linked to each other and more specifically from which thymine the bridging methylene group is derived (Figure 1). These assignments were carried out in the following way. The proton H_{6b} is linked to sugar B as shown by the cross-peak between H_{6b} and $C_{1'B}$ and between $H_{1'B}$ and $(C{=}O)_{2b}$ (Figures 2A and 2B, respectively). Then sugar B is linked to the phosphate group from the carbon $C_{5'B}$ as evidenced by the interaction between protons $H_{5'B/5''B}$ and the phosphorus atom (Figure 3). The phosphate group is linked to sugar A by carbon $C_{3'A}$ (interaction between P and $H_{3'A}$, Figure 3). Finally, the anomeric proton $H_{1'A}$ is linked to the base bearing the unmodified methyl group (correlations between $H_{1'A}$ and

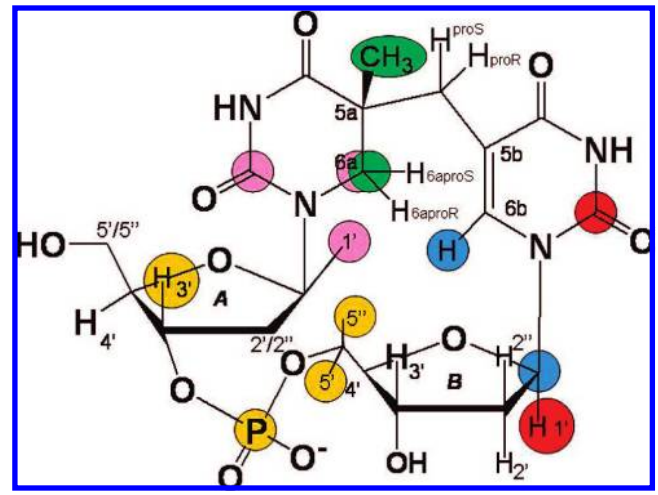

Figure 4. Structure of SPTpT indicating the through-bond correlations used to determine the enchainment of different chemical groups (thymine, sugar, and phosphate). Different colors were used to specify each group of coupled protons.

$(C{=}O)_{2a}$, $H_{1'A}$ and C_{6a} as well as CH_3 and C_{6a}, Figures 2C and 2D, respectively). Figure 4 summarizes all these through-bond correlations. Combined together, these results unambiguously demonstrate a 5′→ 3′ dinucleotide structure and exclude a 3′→5′ one (Figure 1A).

As a striking feature, the H_{6a} protons are isochrone when the SPTpT is dissolved in D_2O, leading to a unique proton singlet at 3.40 ppm. As a consequence, the number of through-space correlations obtained with NOESY experiments was insufficient to allow an unambiguous determination of the absolute configuration of C_{5a} carbon. Therefore, different experimental conditions (temperature, solvent, magnetic field) were tested. Only with DMSO as solvent did the isochrone feature of the two H_{6a} protons disappear.

Absolute Configuration of SPTpT in DMSO-d_6 Determination by NMR. Table 1 shows the results of the complete and unambiguous assignment of proton and carbon chemical shifts obtained when the NMR spectra were recorded in hexadeuteriated DMSO, using the same strategy as in D_2O. In contrast to the NMR experiments in D_2O, the H_{6a} resonance becomes a doublet of doublet at 2.98 and 3.15 ppm corresponding to $H_{6apro\mathit{R}}$ and $H_{6apro\mathit{S}}$ protons, respectively. Thanks to the larger number of through-space correlations in DMSO, the different spin systems corresponding to sugar rings and thymine bases can be unambiguously identified, and the absolute configuration of C_{5a} carbon can be determined as shown below. It should be noted that DMSO is more viscous than D_2O, thus, the $\omega\tau_c$ value (in DMSO) is larger and approaches 1. ROESY experiments were therefore used when SPTpT was dissolved in DMSO. Cross-peaks of the ROESY 2D maps clearly showed that the protons can be separated into two groups on the basis of their through-space correlations. One group can be defined by the protons ($H_{6apro\mathit{R}}$, CH_3, $H_{pro\mathit{S}}$) located in front of a plane defined by the carbon atoms of the thymine ring bearing the methyl group and the second one by protons ($H_{6apro\mathit{S}}$, H_{6b}, $H_{pro\mathit{R}}$) located behind this plane (Figures 5 and 6 and Figure S1 in Supporting Informations). For the protons of the bridging CH_2, the $H_{pro\mathit{S}}$ proton presents a stronger correlation with the methyl group than does the the $H_{pro\mathit{R}}$ proton. The protons $H_{6apro\mathit{S}}$ and $H_{6apro\mathit{R}}$ are discriminated by their ROESY cross-peaks with $H_{2'A/2''A}$ protons. Only $H_{6apro\mathit{S}}$ exhibits a strong interaction with them.

Table 1. ^{1}H and ^{13}C NMR Data of the Dinucleotide Spore Photoproduct Diluted in DMSO and at Room Temperature

identification of proton or carbon	^{1}H chemical shift (ppm)	^{13}C chemical shift (ppm)	$^{1}H-^{13}C$ long-range correlations[a]	$^{1}H-^{1}H$ through-space correlations[b]
H_{proS}/H_{proR}	2.64/2.50	33.12	CH_3 (^3J)−H_{6b} (^3J)	CH_3, H_{6b}
CH_3	1.03	22.21	−	H_{proS}, H_{6aproR}
$H_{6aproS/6aproR}$	3.15/2.98	45.28	CH_3 (^3J)	H_{6aproS}: $H_{2'A}/H_{2''A}$, $H_{3'A}$, H_{6b} H_{6aproR}: $H_{3'A}$, CH_3
$H_{1'A}$	5.99	81.68	−	$H_{2'A}/H_{2''A}$, $H_{4'A}$
$H_{2'A}/H_{2''A}$	2.11	35.21	−	$H_{1'A}$, H_{6aproS}, $H_{3'A}$, $H_{4'A}$
$H_{3'A}$	4.43	73.50	$H_{2'A}/H_{2''A}$ (^2J)	$H_{2'A}/H_{2''A}$, $H_{6aproS/6aproR}$, $H_{4'A}$
$H_{4'A}$	3.41	83.07	−	$H_{3'A}$, $H_{2'A}/H_{2''A}$, $(OH)_A$
$H_{5'A}/H_{5''A}$	3.44	62.36	−	$(OH)_A$
H_{6b}	7.50	138.80	H_{proS}/H_{proR} (^3J)	H_{proS}/H_{proR}, H_{6aproS}
$H_{1'B}$	5.86	84.66	H_{6b} (^3J)	$H_{2'B}/H_{2''B}$, $H_{4'B}$
$H_{2'B}/H_{2''B}$	2.16	40.70	−	$H_{1'B}$, $H_{3'B}$
$H_{3'B}$	4.27	69.92	−	$H_{2'B}/H_{2''B}$, $(OH)_B$, $H_{4'B}$
$H_{4'B}$	3.76	86.06	−	$H_{3'B}$, $H_{1'B}$, $H_{5'B}/H_{5''B}$
$H_{5'B}/H_{5''B}$	3.87	64.51	−	$H_{4'B}$
C_{5b}	−	109.60	H_{proS}/H_{proR} (^2J)	−
C_{5a}	−	40.47	CH_3 (^3J)−NH (^3J)−H_{6aproS} (^2J)	−
$(C{=}O)_{2b}$	−	150.82	H_{6b} (^3J)	−
$(C{=}O)_{4b}$	−	164.10	H_{proS}/H_{proR} (^3J)−H_{6b} (^3J)	−
$(C{=}O)_{2a}$	−	153.36	H_{6aproS} (^3J)	−
$(C{=}O)_{4a}$	−	174.72	$H_{6aproS/6aproR}$ (^3J)−CH_3 (^3J)−H_{proS} (^3J)	−
$(OH)_A$	5.63	−	−	$H_{5'A}/H_{5''A}$, $H_{4'A}$
$(OH)_B$	5.27	−	−	$H_{3'B}$
NH	10.07/7.06	−	−	−

[a] Measured with a HMBC sequence. [b] Measured by 2D ROESY experiments.

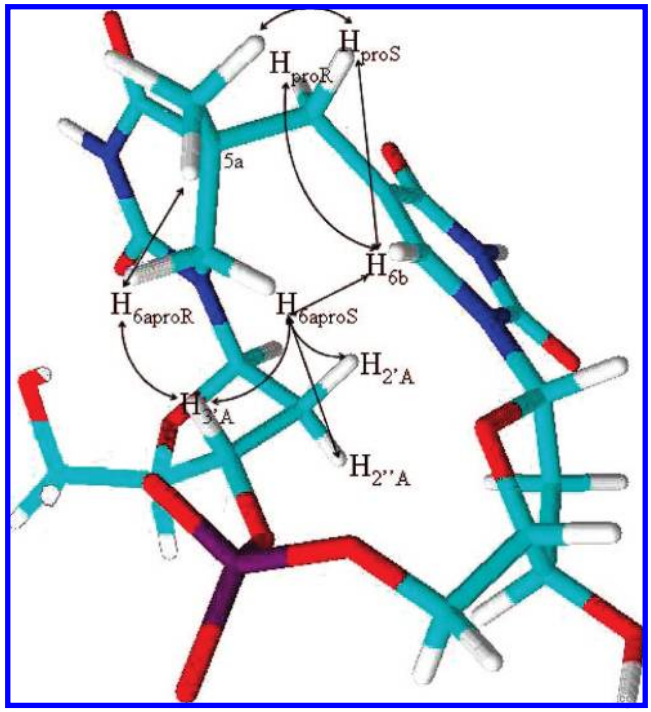

Figure 5. Three-dimensional model showing the main ROESY cross-peaks of the dinucleotide spore photoproduct SPTpT diluted in DMSO used for determining the stereochemistry at C_{5a}. To simplify the figure, only one ROESY correlation has been shown for the methyl group (correlation with a given proton). The protons $H_{2'A}$ and $H_{2''A}$ were annotated randomly.

Furthermore, H_{6aproS} displays a weaker coupling to the methyl group compared to H_{6aproR}. These interactions indicate that the CH_2 group has to be located above the sugar A ring. In addition, the strong interaction between H_{6aproR} and the methyl group unequivocally proves that the configuration of the C_{5a} carbon is *R*. In the case of an *S* configuration, the proton H_{6aproR} could not display at the same time a strong coupling to $H_{3'A}$ and to protons of methyl group. Careful examination of molecular

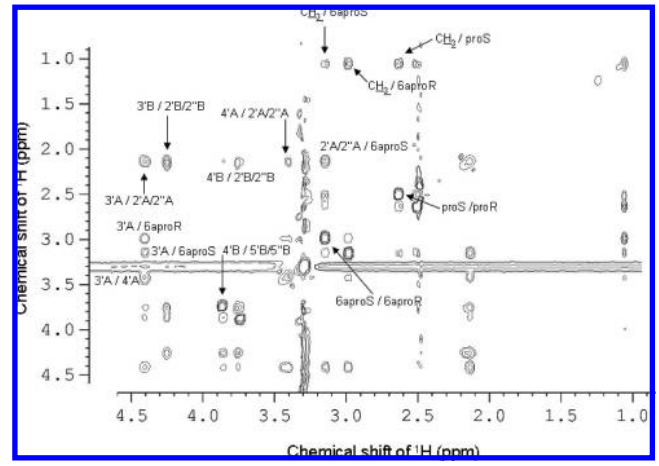

Figure 6. Zoom-in view of the weft-ROESY (mixing time = 300 ms) spectrum of the dinucleotide spore photoproduct SPTpT diluted in DMSO used for determining the stereochemistry at C_{5a}.

models indicates that it would be impossible to obtain the same correlation patterns within each of the two protons groups for an *S* configuration at C_{5a}.

For a spore photoproduct dinucleoside without the phosphodiester bridge, Carell et al.[24] used NOESY cross-peaks to highlight two groups of protons interacting together. Discrimination for the determination of the C_{5a} carbon stereochemistry was based only on the coupling between the methyl group and H_{6a} protons. In our study, we observed two additional correlations involving H_{6a} protons, namely between H_{6aproS} and $H_{2'A/2''A}$ and between H_{6aproS} and H_{6b}. The absence of a phosphodiester bridge in Carell's compound increases the flexibility of synthesized TpT and explains the absence of these two additional couplings. Accordingly, Carell et al.[10] observed many more

(24) Friedel, M. G.; Berteau, O.; Pieck, J. C.; Atta, M.; Ollagnier-de-Choudens, S.; Fontecave, M.; Carell, T. *Chem. Commun.* **2006**, 445–447.

cross-peaks by investigating a SP analogue with a bulky alkyl chain bridging the two sugars.

Conformational Features of Sugars Using the NMR Coupling Constants. In order to complete the structural characterization of the spore photoproduct SPTpT, we have incorporated some conformational considerations on 2-deoxyribose, using the classical interpretation of coupling constants. There are twenty possible conformers for the furanose cycle depending on whether one (E form) or two atoms (T form) of this cycle are outside the plane drawn up by it. As previously described,[25,26] it is possible to identify the type of conformer using coupling constants. Sundaralingam et al.[25] have shown that a $(J_{1'2'} + J_{1'2''})$ value ranging from 7.1 to 16.1 Hz is characteristic for the C2′-endo conformation. In our case, the value of $(J_{1'2'} + J_{1'2''})$ is about 11.7 Hz for sugar A and approximately 15.1 Hz for sugar B. Both sugars of our dinucleotide spore photoproduct SPTpT therefore present a C2′-endo conformation. This result is not surprising since sugars in nucleic acids preferentially adopt either the C3′-endo (North) or C2′-endo (South) conformations. The latter is the most common in solution. However, it is interesting to note that the conformation of sugars in our compound does not appear to be affected by structural constraints induced by the two cross-linked bases.

Comparison between Theoretical and NOE Experimental Interproton Distances. Calculations of interatomic distances were made on the two possible diastereoisomers of this compound exhibiting either an *R* or an *S* configuration at the C_{5a} atom. A requisite to such calculations was the availability of realistic geometries. Using a molecular mechanic approach (COSMOS[11−13]), two structures with the lowest energies were retained for each diastereoisomer. These four structures were further geometry-optimized by DFT calculations, and the more stable geometry for each diastereoisomer was selected. It should be noted that these final structures are degenerated. The calculated distances within SPTpT were then compared to those that could be inferred from the NOESY and ROESY experiments (Table S2 and Figure S2 in Supporting Informations). In contrast to what we have obtained in previous studies using the same strategy on other modified nucleotides,[27−31] several discrepancies appeared between the theoretical and experimental distances. These difficulties can arise from the complexity of the spin system where the protons are strongly interconnected through dipolar coupling and no longer fulfill the approximation of isolated spin pairs for the mixing times that we used in the study. Accordingly, it was not possible to calculate distances using mixing times shorter than 50 ms because the signal-to-noise ratio 2D maps, recorded with shorter mixing time, do not make quantitative measurements.[32−36] Furthermore, whereas the methyl group is very important for the distance constraints, its free rotation is likely to alter the measurement of dipolar interactions with other protons.

Table 2. Comparison of Theoretical and Experimental $^1H-^1H$ Correlations Used to Check the Stereochemistry at C_{5a}[a]

distances	theoretical correlations strength of diastereoisomer *R*	theoretical correlations strength of diastereoisomer *S*	ROESY cross-peaks strength
$H_{6b}-H_{pro\mathit{S}}$	f	f	**R**
$H_{6b}-H_{pro\mathit{R}}$	**F**	f	R
$H_{6b}-H_{5a}$	f	F	−
$H_{6b}-H_{6apro\mathit{S}/\ 6apro\mathit{R}}$	F/f	F/f	R/−
$H_{6b}-H_{2'B}$ or $H_{2''B}$	f/f	f/f	r
$H_{6b}-H_{2'A}$ and $H_{2''A}$	F/f	f/f	**R**
$H_{pro\mathit{R}}-H_{5a}$	f	F	r
$H_{pro\mathit{R}}-H_{6apro\mathit{S}/6apro\mathit{R}}$	F/f	f/f	−/−
$H_{pro\mathit{S}}-H_{5a}$	F	f	**R**
$H_{6apro\mathit{S}/6apro\mathit{R}}-H_{5a}$	F/F	F/f	r/**R**
$H_{6apro\mathit{S}/\ 6apro\mathit{R}}-H_{1'A}$	f/f	f/f	−/−
$H_{6apro\mathit{S}}-H_{2'A/2''A}$	F	F	**R**
$H_{6apro\mathit{R}}-H_{2'A/2''A}$	f	f	−
$H_{6apro\mathit{S}/6apro\mathit{R}}-H_{3'A}$	**F**/F	**F**/F	R/R

[a] For theoretical distance <2.5 Å → correlation strength = **F**; for 2.5 Å < theoretical distance <3.5 Å → correlation strength = F; for theoretical distance > 3.5 Å → correlation strength = f. Strong ROESY cross-peak = **R**; medium ROESY cross-peak = R; weak ROESY cross-peak = r.

Therefore, a qualitative approach was used to overcome this difficulty. For both optimized geometries, the theoretical distances were used to define three different ranges (weak, medium, and strong) of correlation intensities. These data were then compared with experimental correlation intensities from ROESY experiments. The results show that the agreement between theory and experiment is greater in the case of the *R* isomer (Table 2). As a matter of fact, about ten correlations favor the *R* isomer against seven for the *S* isomer. On the basis of this truth table, the privileged absolute configuration would be *R*.

Proton and Carbon Chemical Shift Calculations. In order to further establish the absolute configuration of the C_{5a} atom, previously optimized geometries were used to predict NMR features. In particular, DFT methods were used to calculate proton and carbon chemical shifts. For the two optimized structures, the calculations were limited to the carbons and protons that are expected to be directly affected by the configuration at C_{5a}. The theoretical chemical shifts are reported in Table 3. For comparison, the theoretical values are plotted versus the experimental ones (Figure 7 (in DMSO) and Figure S3 (in D_2O) in Supporting Informations). This clearly shows that, whatever the solvent and the type of atom (carbon or proton), only the theoretical values found for the structure with an *R* configuration at C_{5a} are in agreement with experimental data, thus confirming the absolute configuration of the asymmetric carbon. For the ^{13}C nuclei, notice in particular the very large discrepancies between experimental and (*S* isomer) theoretical data for three out of five nuclei whereas the agreement is satisfactory for all nuclei in the *R* isomer. Similar remarks apply to the case of proton nuclei. Root mean square deviations can be computed for both solvents, nuclei, and isomers. In D_2O, we have rms (^1H, R) = 0.27 ppm against 1.15 ppm for rms (^1H, S) (0.47 against 1.24 ppm in DMSO,

(25) Altona, C.; Sundaral, M. *J. Am. Chem. Soc.* **1972**, *94*, 8205–8212.
(26) Cheng, D. M.; Sarma, R. H. *J. Am. Chem. Soc.* **1977**, *99*, 7333–7348.
(27) Ammalahti, E.; Bardet, M.; Molko, D.; Cadet, J. *J. Magn. Reson. Ser. A* **1996**, *122*, 230–232.
(28) Reggelin, M.; Hoffmann, H.; Kock, M.; Mierke, D. F. *J. Am. Chem. Soc.* **1992**, *114*, 3272–3277.
(29) Bougault, C.; Jordanov, J.; Bardet, M. *Magnetic Resonance In Chemistry* **1996**, *34*, 24–32.
(30) Ammalahti, E.; Bardet, M.; Cadet, J.; Molko, D. *Magn. Reson. Chem.* **1998**, *36*, 363–370.
(31) Bombelli, C.; Borocci, S.; Lupi, F.; Mancini, G.; Mannina, L.; Segre, A. L.; Viel, S. *J. Am. Chem. Soc.* **2004**, *126*, 13354–13362.
(32) Cano, K. E.; Thrippleton, M. J.; Keeler, J.; Shaka, A. J. *J. Magn. Reson.* **2004**, *167*, 291–297.
(33) Thrippleton, M. J.; Keeler, J. *Angew. Chem., Int. Ed.* **2003**, *42*, 3938–3941.
(34) Bax, A. *J. Magn. Reson.* **1988**, *77*, 134–147.
(35) Esposito, G.; Pastore, A. *J. Magn. Reson.* **1988**, *76*, 331–336.
(36) Olejniczak, E. T.; Gampe, R. T.; Fesik, S. W. *J. Magn. Reson.* **1986**, *67*, 28–41.

Table 3. Experimental ^{1}H and ^{13}C Chemical Shifts (D_2O and DMSO) and Theoretical ^{1}H and ^{13}C Chemical Shifts (*R* and *S* configurations) of the Dinucleotide Spore Photoproduct SPTpT

identification of proton or carbon	^{1}H chemical shift (ppm)				^{13}C theoretical chemical shift (ppm)			
	experimental		theoretical		experimental		theoretical	
	D_2O	DMSO	*R*	*S*	D_2O	DMSO	*R*	*S*
$H_{pro\,S}/H_{pro\,R}$	2.97/2.50	2.64/2.50	2.3/3.2	1.3/1. 7	37	33.12	34.7	84.2
CH_3	1.30	1.03	1.40	3.3	23.56	22.21	20.5	33.1
$H_{6apro\,S/6apro\,R}$	3.40	3.15/2.98	3.2/3.7	3.4/4.2	45.71	45.28	46.9	49.1
H_{6b}	7.76	7.50	8.2	8.2	138.86	138.80	141.2	110.4
C_{5a}	–	–	–	–	40.27	40.47	46.5	44.5

respectively), as well as rms (^{13}C, R) = 3.47 ppm against 25.13 ppm for rms (^{13}C, S) (3.17 against 26.70 ppm in DMSO, respectively). The *R* isomer is therefore unambiguously established.

In conclusion, the full characterization of the dinucleoside monophosphate SPTpT (in two solvents) was accomplished through the NMR measurements and theoretical calculations, and it has been obviously shown that carbon C_{5a} presents an *R* absolute configuration.

Discussion

The present work is the first complete characterization of the natural spore photoproduct SPTpT, using NMR spectroscopy in D_2O and DMSO-d_6 and theoretical calculations. The compound studied here was obtained in pure form by UV irradiation of the TpT dimer and was previously found to be identical to that obtained by irradiation of DNA under comparable conditions followed by enzymatic hydrolysis.[8] In both cases, only one diastereoisomer was produced during the reaction as shown by HPLC and, in the present study, by NMR spectroscopy. Furthermore, this compound is efficiently changed into two unmodified thymines by the repair enzyme spore photoproduct lyase.[8] Our present study firmly establishes that SPTpT has the structure shown in Figure 1A (*R* isomer), with the following characteristics: (i) a 5′→3′ dinucleotide structure; (ii) the configuration of the asymmetric C_{5a} carbon is *R*. These unambiguous results illustrate the efficiency of the applied strategy combining spectroscopic analyses and DFT calculations for structural assignment of complex molecules.

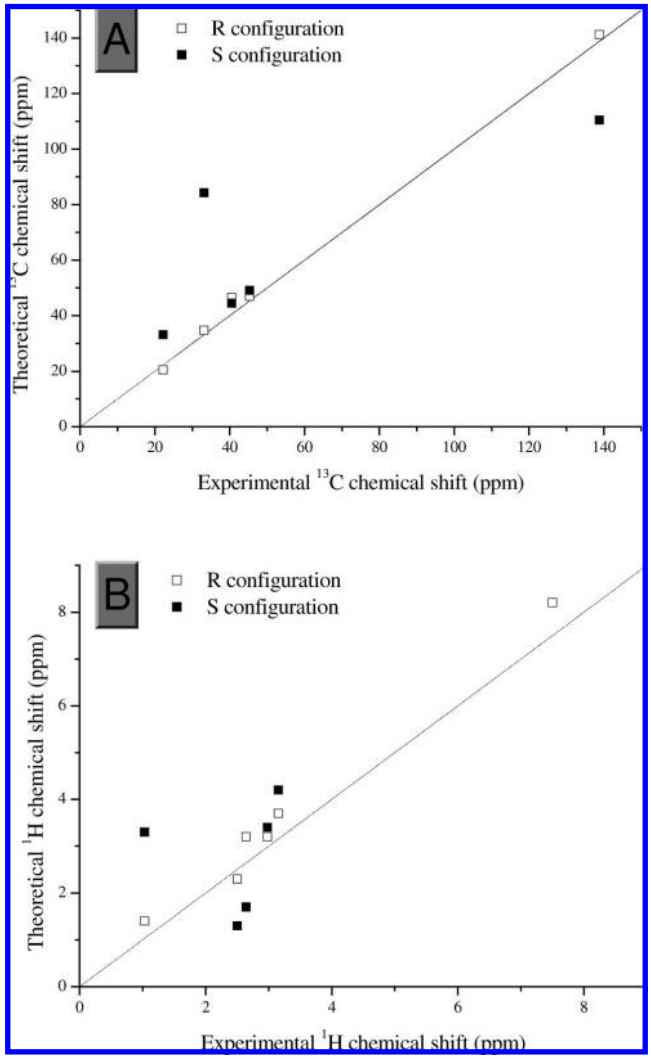

Figure 7. Theoretical chemical shift as a function of experimental chemical shift for ^{13}C (A) and ^{1}H (B) of the dinucleotide spore photoproduct SPTpT diluted in DMSO. In B, the point at 7.50 ppm is the same for both configurations.

Very interestingly, the presently determined structure for SPTpT is also consistent with several other observations. First, reactions between thymine radicals and adjacent nucleosides within double-stranded DNA have been shown to be favored when thymine was on the 3′-end. These observations were rationalized in terms of shorter distances between the adjacent 5′-end base and the C_5, C_6, or methyl of the thymine moiety.[37,38] Although experiments involving labeled thymine pointed to a concerted rather than a radical mechanism,[39] similar considerations are likely to explain why the methylene link between the two thymine rings of SP involves the methyl group of the 3′-end base (for conformation A of DNA: C−C distances between $Me_{3'}$ and $C_{5'}$ = 3.69 Å and between $Me_{5'}$ and $C_{3'}$ = 5.52 Å). The absolute configuration of the C_{5a} atom also reflects structural features of DNA. Indeed, pyrimidine nucleotides display an anti conformation of the bases with regard to deoxyribose. These constraints impose that the natural isomer of the spore photoproduct should be the one with an *R* configuration at C_{5a}, as previously suggested by Begley.[9] Therefore, our structural assignment of SPTpT is also in agreement with that expected from the known conformation of DNA. The observation that the presently studied photoproproduct is completely repaired by the spore photoproduct lyase further emphasizes that the determined configuration reflects natural structural features of DNA.[8]

Two studies from T. P. Begley's[9] and T. Carell's[10] groups had previously addressed this configuration issue. Here, we will discuss only the former since only in this case was the same SPTpT compound investigated. Begley et al.[9] described a synthetic route to the dinucleoside monophosphate spore photoproduct. The two 5′ →3′ diastereoisomers, with either an *R* or an *S* configuration at carbon C_{5a}, were prepared and

(37) Bourdat, A. G.; Douki, T.; Frelon, S.; Gasparutto, D.; Cadet, J. *J. Am. Chem. Soc.* **2000**, *122*, 4549–4556.
(38) Bellon, S.; Ravanat, J. L.; Gasparutto, D.; Cadet, J. *Chem. Res. Toxicol.* **2002**, *15*, 598–606.
(39) Cadet, J.; Vigny, P. *The photochemistry of nucleic acids*; 1990; Vol. 1.

characterized by NMR spectroscopy in D_2O under conditions comparable to those used in the present study. As expected, one of these isomers exhibits ^1H chemical shifts almost identical to those of the SPTpT compound studied here. According to Begley's work, this product is the *S* isomer whereas we clearly established that the absolute configuration at C_{5a} is *R*. Without taking into account this discrepancy in the absolute configuration determination, the ^1H NMR assignments were also identical between the two studies, with the exception of protons $H_{1'A}$, $H_{1'B}$ on one hand and $H_{2'A/2''A}$, $H_{2'B/2''B}$ on the other hand. We believe that the assignments proposed by Begley's group were incorrect since our data (NMR 2D $^1H-^{13}C$ HMBC and TOCSY experiments) allowed us to unambiguously assign the anomeric protons of sugars A and B and consequently $H_{2'/2''}$ protons which are coupled to them (correlations between $C_{1'B}$ and H_{6b} and between $H_{1'B}$ and $(C{=}O)_{2b}$, respectively Figures 2A and 2B). The origin of the discrepancy about the absolute configuration of C_{5a} is unclear, but our detailed NMR analysis (including the truth table, Table 2) and the good agreement between experimental and calculated ^{13}C and ^1H NMR chemical shifts (Table 3 and Figure 7) strongly suggest an incorrect configuration assignment in the previous study. Besides, it is worth reminding that the determination of absolute configuration is not something obvious but rather a difficult task to carry out.

Conclusions

The disagreement between our assignment of the configuration of SPTpT and those previously reported led us to realize a very extensive study combining NMR and DFT techniques, leading us to conclude an *R* absolute configuration of the 5′→3′ SPTpT dinucleotide. In previous work,[40−43] a quite classical approach consisting of two steps was used. First, interatomic distances were estimated from NOESY and ROESY experiments. These distances were then used as constraints in a molecular mechanical calculation. A distance matrix was constructed, containing upper and lower distance bounds, and various structures were searched for which satisfied these constraints. Finally, potential energy terms were introduced, and the geometries yielding the lowest energies were selected. Motivated by the fact that the experimental and theoretical distances are not comparable, we proceeded otherwise. We alternatively optimized by DFT means the "best" geometries obtained for *R* and *S* conformations by standard molecular mechanics without constraints and further computed the NMR proton and carbon chemical shifts. Figure 7 shows clearly that only theoretical ^1H and ^{13}C chemical shifts of the *R* configuration are in agreement with the experimental results, although these calculations have been performed in vacuum without solvent effects. In return, some of the distances determined from NMR data alone differ greatly from the geometry-optimized distances. It can be verified in Figure S2 and Table S2 in Supporting Informations that the NMR distances are systematically shorter than the DFT distances. Some suggestions on the experimental side, explaining these disagreements, have been proposed previously. Consequently, great caution should be exerted when determining experimental geometries from NMR distance constraints only, for systems characterized by an intermediate $\omega\tau_c$ regime.

Supporting Information Available: ^1H and ^{13}C NMR data and theoretical and experimental distances of the SPTpT diluted in D_2O. Weft-ROESY of SPTpT diluted in DMSO. Theoretical distances as a function of experimental distances, and theoretical chemical shifts as a function of experimental chemical shift for ^{13}C and ^1H of SPTpT diluted in D_2O. HPLC-MS/MS chromatogram of TpT exposed to UVC in the presence of DPA-Na. This material is available free of charge via the Internet at http://pubs.acs.org.

JA805032R

(40) Koning, T. M. G.; Davies, R. J. H.; Kaptein, R. *Nucleic Acids Res.* **1990**, *18*, 277–283.
(41) Zhao, X. D.; Nadji, S.; Kao, J. L. F.; Taylor, J. S. *Nucleic Acids Res.* **1996**, *24*, 1554–1560.
(42) Blommers, M. J. J.; Lucasius, C. B.; Kateman, G.; Kaptein, R. *Biopolymers* **1992**, *32*, 45–52.
(43) Clivio, P.; Favre, A.; Fontaine, C.; Fourrey, J. L.; Gasche, J.; Guittet, E.; Laugaa, P. *Tetrahedron* **1992**, *48*, 1605–1616.